CHAPTER VII

ELECTROPHORETIC DEPOSITION OF EXFOLIATED GRAPHENE OXIDE (eGO)

Chapter Overview

Knowing that exfoliated graphene oxide (eGO) can form aqueous suspensions, we sought to investigate the colloidal stability of these suspensions. The stability was assessed using electrophoretic mobility measurements, from which the zeta potential was calculated. Tuning over the pH range 2 to 12, we identified three suspension regimes: (1) high stability, high conductivity, (2) high stability, low conductivity, and (3) moderate stability, high conductivity. With these three suspension regimes, we performed a set of electrophoretic deposition (EPD) survey experiments using different voltage and time parameters to gain insight on the different suspension regimes' deposition behavior. Armed with a greater understanding of eGO deposition from the survey experiments, we identified EPD conditions to use as we subsequently investigated the preparation of the free-standing eGO films.

7.1 Tuning eGO Suspensions

The centrifuged eGO suspensions in water (concentration 0.92 mg/ml, described in Section 6.4) were diluted to a concentration of 0.35 mg/ml for the EPD experiments. The zeta potential of colloids in aqueous suspensions can be altered readily by the addition of salts, acids, or bases. The presence of these charges also alters the conductivity of the suspension. To study our suspensions at different pH values, we measured the electrophoretic mobility and conductivity using the Malvern Zetasizer. The pH values of the suspensions were measured using a Denver Instrument UP-10 pH meter. The zeta potential was calculated from the mobility using the Smoluchowski approximation. We prepared eGO suspensions over a wide range of pH values by titration of HCl or KOH solutions in water. Figure 7-1 shows the zeta potential and conductivity of the eGO suspensions plotted as functions of measured pH value.

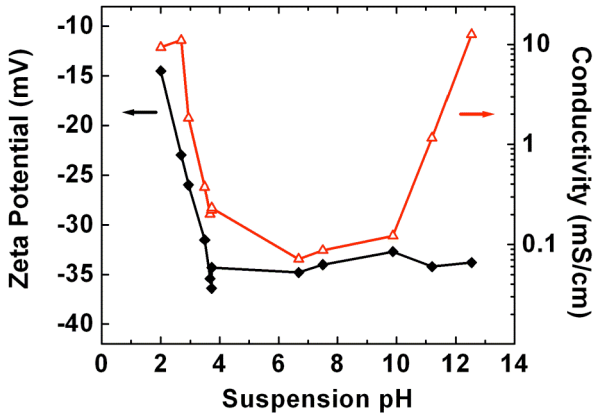

Figure 7-1. Zeta potential and conductivity of eGO suspension, as a function of measured pH value. Lines are a guide for the eye. (Measurement error: pH ± 0.1, zeta potential ± 1 mV, conductivity ± 2%)

The conductivity exhibited a minimum value at pH ~ 7, which is reasonable given that neutral-pH deionized water does not contain an uncompensated excess of H+ or OH- ions, or in other words, [H+] = [OH-]. As the suspension pH moved away from 7 toward more acidic or more basic values, the conductivity increased, reflecting the presence of a greater quantity of ions, either H+ or OH- and the respective counter-ion, Cl- or K+. As the pH transitioned from 10 to 12 and from 4 to 2, we observed that the conductivity increased almost two orders of magnitude. This observation was sensible given that a change of 1 in pH value corresponds to a 10-fold increase in the concentration of H+ or OH- ions. The conductivity plot is shaped more like the letter ‘U’ than the letter ‘V’ because some of the ions added to the suspension, to move the pH away from 7, joined the double layer surrounding the eGO colloids and did not contribute as strongly to the suspension conductivity.

In the pH range that we probed, the zeta potential exhibited values ranging from -15 mV to -35 mV. The colloids’ negative charge (indicated by the negative sign of the zeta potential) likely originated from the carboxylate groups on the eGO sheet edges, whose presence was indicated by the infrared spectroscopy measurement in Section 6.2.4. The zeta potential reflected stable suspensions (magnitude > 30 mV) at pH ≥ 3.6. In Figure 7-2, we visually compare suspensions with zeta potential -15 mV and -35 mV. The -15 mV suspension exhibited

floccing, with the formation of aggregates that remained afloat in the suspension. The -35 mV suspension, meanwhile, remained free of visible aggregation. These observed suspension behaviors corroborated the interaction energy calculation displayed in Figure 2-6, which suggested that graphene colloids with zeta potential of -15 mV would possess a very low energy barrier to aggregation at room temperature.

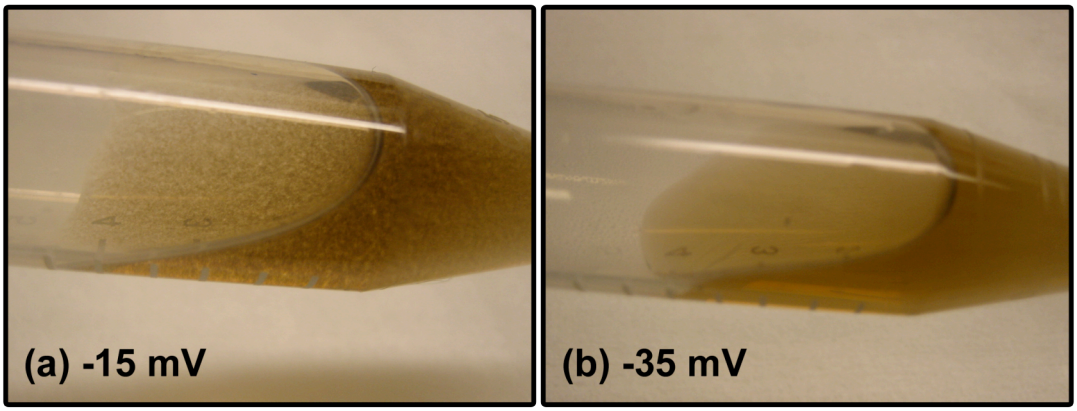

Figure 7-2. Photographs of eGO suspension with zeta potential of (a) -15 mV and (b) -35 mV. Flocs (aggregates) visible in (a) are absent in (b).

We tested the validity of using the Smoluchowski approximation by comparing the lateral dimension of an eGO sheet to the Debye length of the suspension present around it. Debye length was calculated using Equation (2.6) given that we knew the concentration of ions that were added to the suspensions. In our eGO suspensions, the Debye length was in the range 3.1 nm to 12.3 nm. This range of values is at least one order of magnitude smaller than the lateral dimension of an eGO sheet (in the range 100 nm to 1000 nm, per Section 6.4), justifying our use of the Smoluchowski approximation to determine zeta potential.

For the EPD experiments, we designated the suspension to have three regimes: (1) high stability, high conductivity, (2) high stability, low conductivity, and (3) moderate stability, high conductivity (Figure 7-3). The 30-mV zeta potential magnitude was designated as the threshold between high stability and moderate stability, as mentioned in Chapter 2. Table 7-1 provides characterization of the suspension regimes used in the subsequent EPD trials.

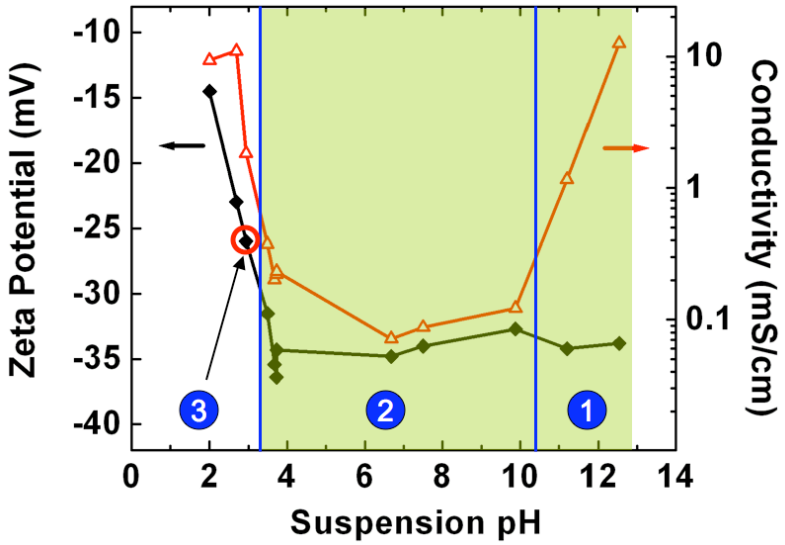

Figure 7-3. The different eGO suspension regimes. The shaded region indicates all suspensions with zeta potential magnitude > 30 mV. Regime 1: High stability, high conductivity. Regime 2: high stability, low conductivity. Regime 3: Moderate stability, high conductivity.

Table 7-1. Properties of the suspension regimes used for the EPD experiments.

	Regime 3	**Regime 2**	**Regime 1**
Suspension pH	2.80 ± 0.02	6.01 ± 0.01	11.53 ± 0.11
Zeta Potential (mV)	-25.7 ± 0.6	-33.4 ± 1.7	-35.0 ± 1.9
Conductivity (mS/cm)	1.70 ± 0.07	0.0752 ± 0.0042	1.04 ± 0.07

7.2 Electrophoretic Deposition Survey Experiments

This section details the EPD survey experiments on the three different eGO suspensions. The objective of these experiments was to garner an understanding of the deposition behavior of eGO films. With this understanding, we could identify the EPD parameters that produced coherent films of eGO, whose “bulk” properties we would investigate subsequently. Therefore, in this survey, films were evaluated by their homogeneity, coverage of the substrate, and microstructure. At a minimum, to be considered “a film” in our experiments, the deposit needed to be visible to the naked eye.

The films were deposited on 0.1-mm thick 316L stainless steel (McMaster Carr) that was cut into 1.5 cm x 3 cm electrodes. Prior to the experiments, the electrodes were sonicated in acetone and rinsed in deionized water. The electrodes were mounted vertically with spacing 5 mm. The setup is shown in Figure 7-4. A BK Precision 1787B power supply was used to apply dc voltage, while we tracked the current using a Keithley 2010 Multimeter. The morphology of films on the electrodes was evaluated by scanning electron microscopy (SEM) using a Hitachi S-4200 microscope operated at 1 kV and 5 kV. The thickness of the films was evaluated using a Veeco Dektak 150 profilometer. (Note about thickness measurements: If the film on the steel had thickness < 300 nm, it was not possible to make an accurate thickness measurement using the profilometer because the film thickness was comparable to the height of the striations in the steel surface. For these samples, we estimated the thickness by SEM. This hindrance reinforced the importance of being able to create free-standing nanoparticle assemblies that can be studied without substrate interference.)

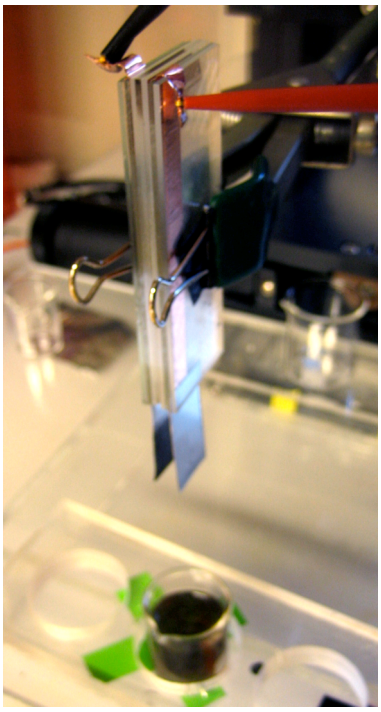

Figure 7-4. Photograph of the EPD setup for the eGO experiments. The parallel steel electrodes await submersion in an eGO suspension.

We wished to study the effects of varying the voltage and the duration of the EPD runs. In the following subsections, we describe the outcome for each set of EPD parameters. At the end of each subsection, a table summarizes the outcome of each experiment.

7.2.1 Low Voltage (0.5 V and 3 V, 5 min)

Parameters — In the first set of trials, 0.5 V was applied for 5 min with the electrodes in the suspension (9 ml liquid volume, 10-ml beaker). The electrodes were withdrawn from the suspension and kept in a horizontal position at 0.5 V for 5 min.

Current — The EPD current from these trials is shown in Figure 7-5. The starting current in each trial is proportional to the conductivity of the suspension used. In all three trials, the current exhibited a decline during the deposition. This decline could have originated from a decrease in ion concentration and/or the formation of a double layer of ions at the electrode surface that increased the resistance at the electrode. The current was sustained by neutralization of some of the ions at the electrode.

Suspensions — The suspensions maintained their light brown, aggregate-free appearance after the EPD runs. Their pH values after the EPD runs were altered by less than 0.05 from their before-EPD values, which is within the instrument error range.

Films — The electrodes from these trials are shown in Figure 7-6. No deposit was visible. In tandem with the decline in current, the lack of deposit would suggest the formation of an ionic double layer at the electrode surface, which the eGO colloids were unable to penetrate.

Parameters — In the second set of these low voltage trials, 3 V was applied for 5 min with the electrodes in the suspension (9 ml liquid volume, 10-ml beaker). The electrodes were withdrawn from the suspension and kept in a horizontal position at 3 V for 5 min.

Current — The EPD current from these trials is shown in Figure 7-5. Even though the voltage was increased 6-fold, the currents in each of these runs increased by significantly more than 6× their counterparts from the 0.5 V trials. Additionally, the currents did not decline continuously during the runs. Instead, they leveled off and increased slightly by the end of the

runs. This current behavior suggested the existence of electrochemical effects, namely the electrolysis of water. At the positively biased electrode, water would be decomposed to yield oxygen gas and dissolved H+ ions. At the negative electrode H+ would combine with electrons to produce hydrogen gas. These gases would be observed as bubbles evolving from the electrode surfaces.

Suspensions — During the run in suspension regime 1, a few bubbles were observed. No bubbles were observed during the runs in regimes 2 and 3. The absence of observation did not indicate actual absence since it was possible that the evolving gas dissolved in the aqueous suspension without forming visible bubbles. In regime 1 the pH decreased by 0.12 while it increased in regimes 2 and 3 by 0.07 and 0.16, respectively. The pH decrease in regime 1 suggested net consumption of OH- ions while the pH increases in regimes 2 and 3 suggested net consumption of H+ ions in the respective suspensions.

Films — The electrodes from these trials are shown in Figure 7-7. In all trials, film was formed on the positive electrode. The films for regimes 2 and 3 were continuous, while the film for regime 1 exhibited incomplete regions. As the electrodes were withdrawn from the liquid in regime 1, we observed a skin layer of “unadhered deposit” to remain behind in the liquid. The film thickness for each suspension regime is shown in Table 7-3. For all three regimes, the likely mechanism for the deposition was ion generation. At the positive electrode, the increase in H+ concentration due to electrolysis decreased the electrostatic repulsion between eGO colloids, enabling them to adhere to form the deposit.

The SEM images of the eGO films are shown in Figure 7-8. In the low-zoom images, the striations of the steel were visible because of the thinness of the films. In the high-zoom images, the outlines of overlapping eGO sheets were visible. Apart from intermittent wrinkles, the sheets themselves appeared to lie flat, parallel to the electrode surface.

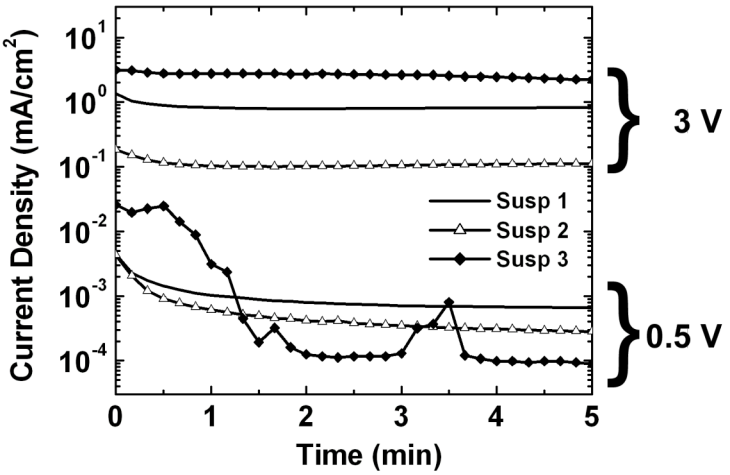

Figure 7-5. Normalized current during 0.5 V and 3 V experiments.

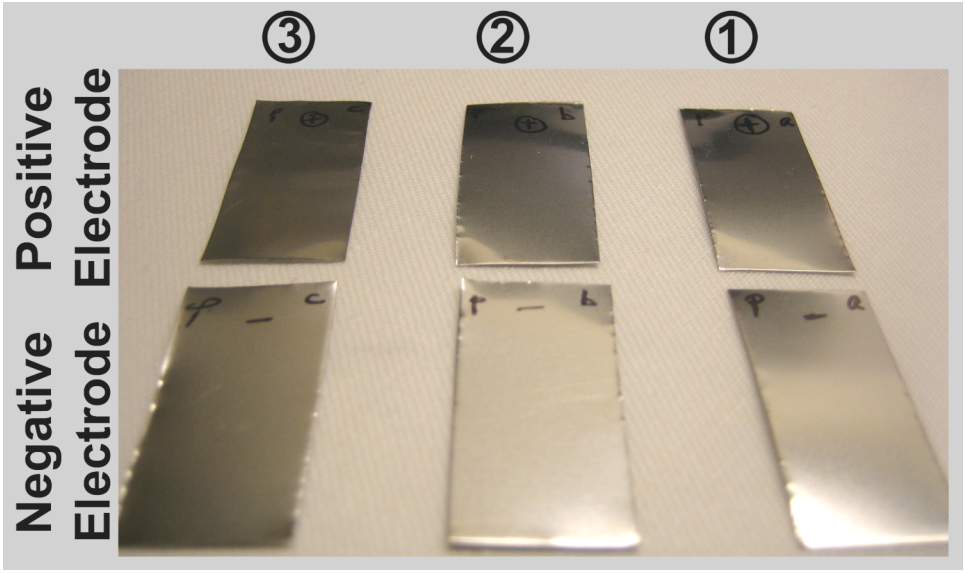

Figure 7-6. Photograph of electrodes from 0.5 V, 5 min experiments.

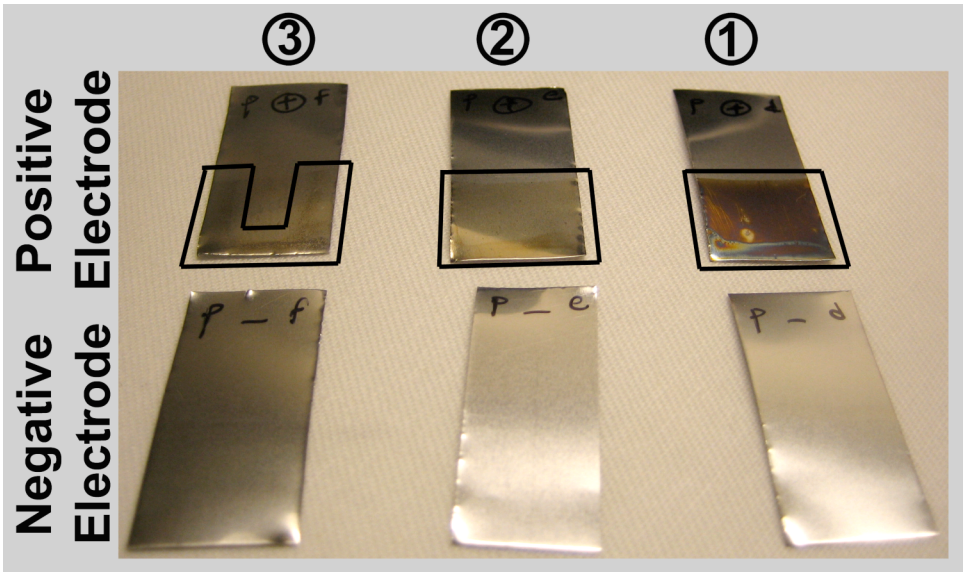

Figure 7-7. Photograph of electrodes from 3 V, 5 min experiments. Lines added as approximate guides to the film boundaries.

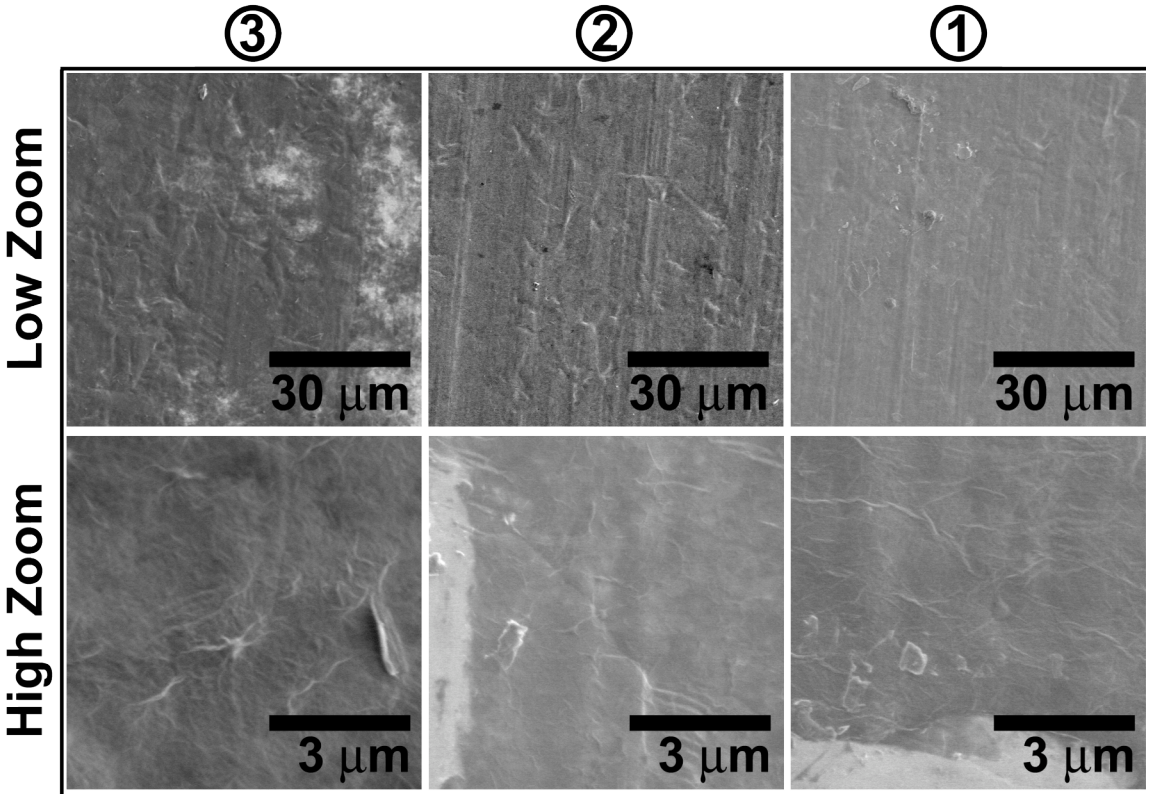

Figure 7-8. SEM images of the films formed in the 3 V, 5 min experiments. The films for all three suspension regimes were on the positive electrode.

Table 7-2. Summary of 0.5 V, 5 min deposition experiments.

	Regime 3	**Regime 2**	**Regime 1**
Film Thickness	No Visible Film	No Visible Film	No Visible Film
Change in Suspension pH	+ 0.03	- 0.05	+ 0.01

Table 7-3. Summary of 3 V, 5 min deposition experiments.

	Regime 3	**Regime 2**	**Regime 1**
Film Thickness	Incomplete Film †	~ 60 nm †, §	~ 230 nm †, §
Change in Suspension pH	+ 0.16	+ 0.07	- 0.12

† Film on positive electrode. § Thickness estimated by SEM.

7.2.2 High Voltage (15 V, 5 min)

Parameters — In this set of trials, 15 V was applied for 5 min with the electrodes in the suspension (9 ml liquid volume, 10-ml beaker). The electrodes were withdrawn from the suspension and kept in a horizontal position at 15 V for 5 min.

Current — The EPD current from these trials is shown in Figure 7-9. Regime 1 maintained roughly the same current value while regimes 2 and 3 exhibited small but steady decreases starting at ~ 2 minutes.

Suspensions — During the runs in suspension regimes 1 and 3, vigorous bubbling was observed at both electrodes. These suspensions flocculated by the end of the runs (Figure 7-10). No bubbling was observed in regime 2. At the end of the run, this suspension appeared free of aggregates, except for a “skin layer” floating at the top (Figure 7-10). Generally, use of higher voltages and their associated current triggered greater ion generation and Joule heating, facilitating the flocculation of the eGO colloids. In regime 1 the pH decreased by 0.21 while it increased in regimes 2 and 3 by 1.24 and 0.47, respectively. The pH decrease in regime 1 suggested net consumption of OH- ions while the pH increases in regimes 2 and 3 suggested net consumption of H+ ions in the respective suspensions.

Films — The electrodes from these trials are shown in Figure 7-11. Similarly to the 3 V experiment, suspension regime 1 yielded a film covering the entire area of the positive electrode that was submerged. Regime 2 yielded sparse regions of film on the positive electrode. Ion generation was the likely mechanism for deposition in these two trials. Regime 3 yielded tiny, sparse spots of material on the positive electrode, but a spotty deposit spanning the entire area of the negative electrode that was submerged. This change in deposition location likely resulted from the generation of H+ in a quantity sufficient to reverse the negative charge of the eGO colloids. In turn, the mechanism for the deposition at the negative electrode would be ion depletion, by the consumption of H+ as it combined with electrons from the electrode while Cl- ions were driven away from the electrode. The steady decrease in the current after ~ 2 minutes supported this assertion.

From SEM in Figure 7-12, we noted that the films from regimes 1 and 2 appeared to have a flat morphology, with some eGO sheets exhibiting wrinkles. In the film from regime 3, there were microscale domains containing flat sheets, and these domains appeared to be stacked with different heights. Interspersed among these domains were voids with area ≤ 10 μm^2. This microstructure suggested that the eGO sheets formed face-to-face adhering multilayers prior to depositing on the electrode (Figure 7-13). That the eGO sheets, possessing negative charge initially, deposited on the negative electrode indicated a reversal from negative to positive charge during the EPD run. The process of reversing colloidal charge is not a discrete flip-the-switch event. In the case of the regime 3 eGO colloids, the colloids' charge (as measured by zeta potential) would have transitioned from -25.7 mV toward positive values with the increase in H+ concentration. As shown in Figure 7-2, the eGO colloids began aggregating at -15 mV. The aggregation would have continued during the transition toward 0 mV due to the further decrease in electrostatic repulsion between the colloids. Because the colloids ended up moving to the negative electrode, we were fairly certain that they acquired at least a small positive zeta potential value prior to deposition. Electrophoretic mobility measurements of the suspension after EPD verified the transition to positively charged colloids (Figure 7-14). Still, once the aggregates of multilayered eGO sheets formed, it would be difficult to separate them because of their strong

van der Waals attractive interaction. Thus, the film contained the microscale domains of flat sheets, with the domains themselves appearing to be stacked on top of one another at different heights.

Because the direction of the eGO colloids' mobility could be reversed when doing deposition from suspension regime 3, we hypothesized that a more filled-in film could be formed on the negative electrode by performing the deposition for a longer time. Therefore, in the next section, we report on EPD at 15 V but for 10 min instead of 5 min.

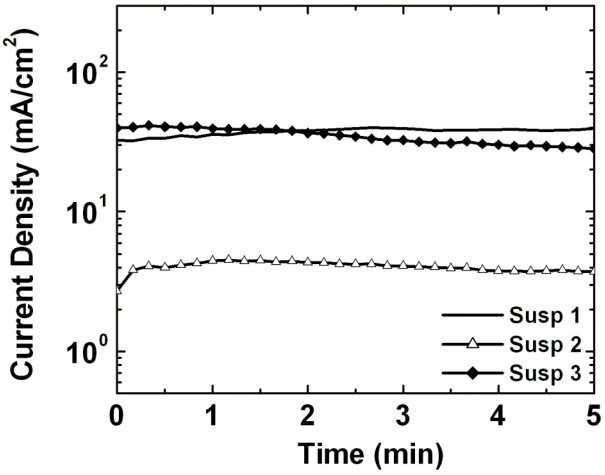

Figure 7-9. Normalized current during 15 V, 5 min experiments.

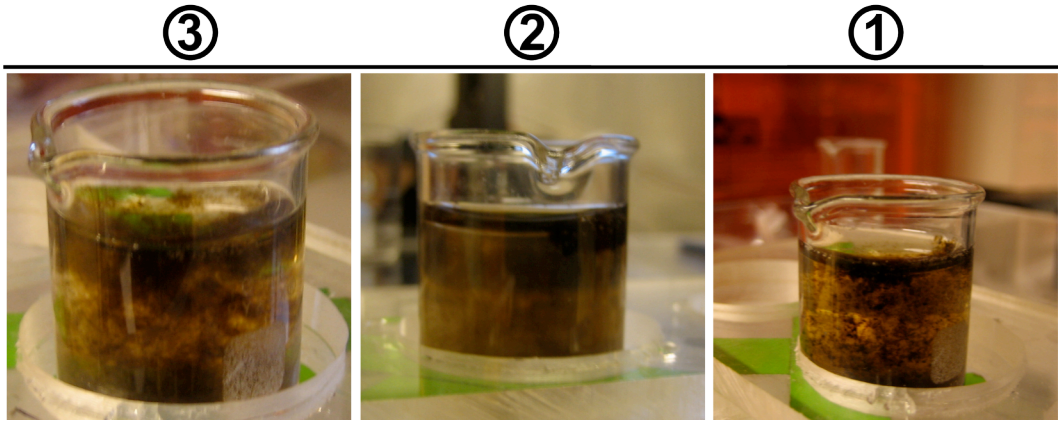

Figure 7-10. Photographs of the three eGO suspension regimes after 15 V, 5 min experiments.

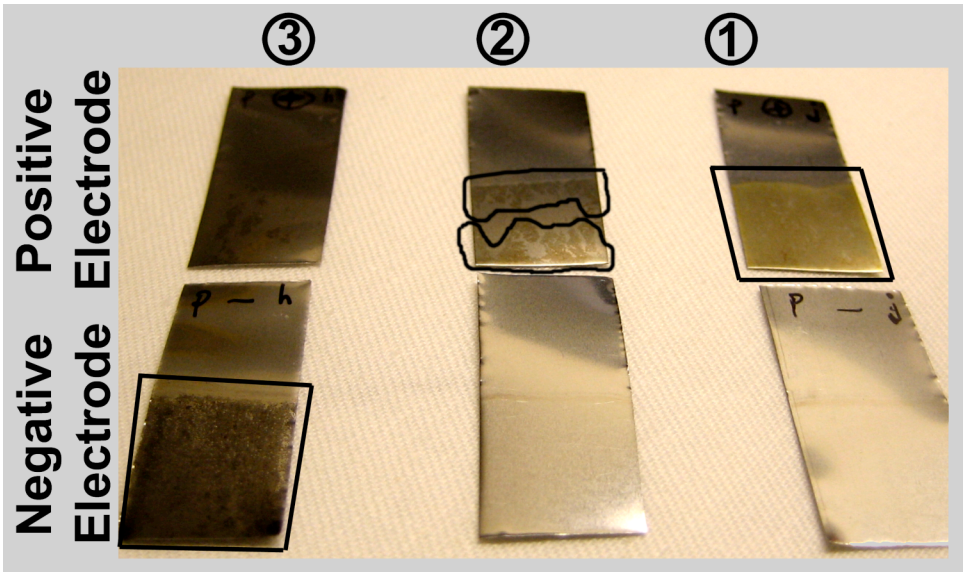

Figure 7-11. Photograph of electrodes from 15 V, 5 min experiments. Lines added as approximate guides to the film boundaries.

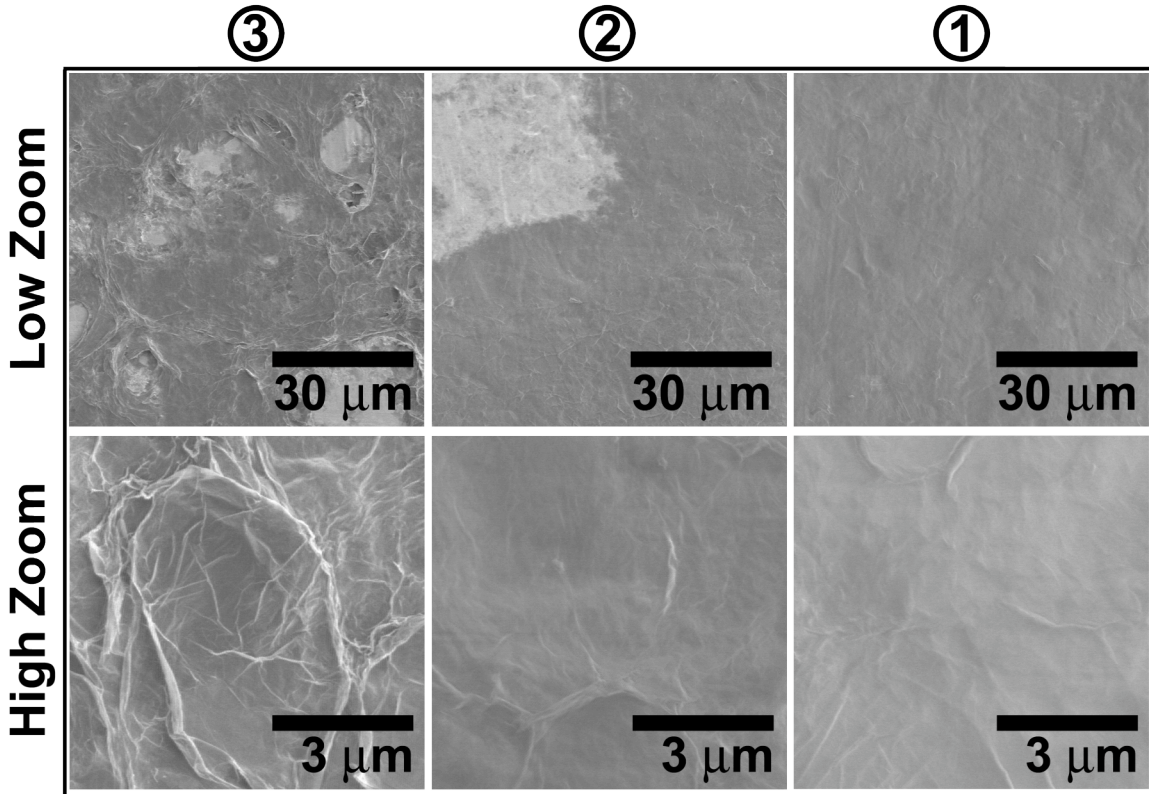

Figure 7-12. SEM images of the films formed in the 15 V, 5 min experiments. The film from suspension regime 3 was on the negative electrode, while the films from regimes 1 and 2 were on the positive electrode.

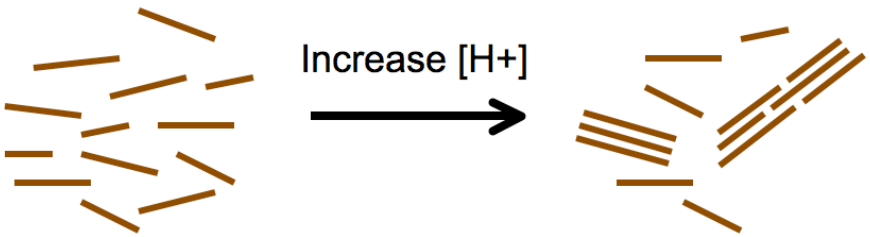

Figure 7-13. Diagram depicting edge view of eGO sheets. An increase in H+ concentration reduces electrostatic repulsion between the negatively charged sheets, leading to increased aggregation. Per calculation of van der Waals interaction energy (Figure 2-4), face-to-face interaction dominates edge-to-edge interaction, leading to formation of aggregates comprising multilayered stacks of eGO sheets.

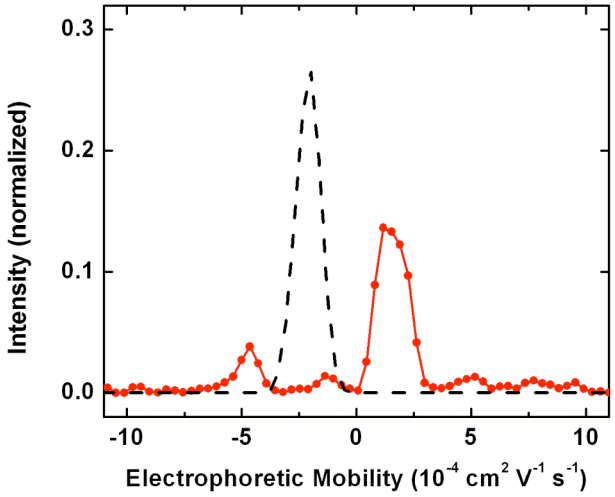

Figure 7-14. Electrophoretic mobility of eGO sheets in suspension regime 3 before (dashed line) and after (solid line with dots) a 15 V, 5 min EPD run.

Table 7-4. Summary of 15 V, 5 min deposition experiments.

	Regime 3	**Regime 2**	**Regime 1**
Film Thickness	Spotty Deposit ‡	Incomplete Film †	469 ± 44 nm †
Change in Suspension pH	+ 0.47	+ 1.24	- 0.21

‡ Film on negative electrode. † Film on positive electrode. § Thickness estimated by SEM.

7.2.3 High Voltage, Extended Time (15 V, 10 min)

Parameters — In this set of trials, 15 V was applied for 10 min with the electrodes in the suspension (8 ml liquid volume, 10-ml beaker). The electrodes were withdrawn from the suspension and kept in a horizontal position at 15 V for 5 min.

Current — The EPD current from these trials is shown in Figure 7-15. The first five minutes appeared consistent with the current from the 15 V, 5 min EPD runs. The current in suspension regime 1 was sustained at ~ 30 mA/cm^2 while the current in regime 2 continued to decrease between 5 minutes and 10 minutes. The current in regime 3 continued to decrease after 5 minutes but eventually leveled off at ~ 20 mA/cm^2 after 7 minutes.

Suspensions — Similarly to the 15 V, 5 min experiments, suspension regimes 1 and 3 exhibited bubbling throughout the EPD runs. By the end of the runs, large flocs were visible in the suspensions. No bubbling was observed in regime 2. In regime 1 the pH decreased by 0.19 while it increased in regimes 2 and 3 by 0.74 and 0.52, respectively. The pH decrease in regime 1 suggested net consumption of OH- ions while the pH increases in regimes 2 and 3 suggested net consumption of H+ ions in the respective suspensions.

Films — The electrodes from these trials are shown in Figure 7-16. Similarly to the 15 V, 5 min experiments, eGO deposited on the positive electrode from regimes 1 and 2 and on the negative electrode from regime 3. The film from regime 1 covered the submerged portion of the electrode completely but the film from regime 2 deposited only in small spots on the electrode, mimicking their respective behavior from the 15 V, 5 min experiments. The film from regime 3, however, exhibited nearly complete coverage of the electrode, an improvement over the spotty deposit that formed in the 15 V, 5 min experiments.

Low and high magnification SEM images of the eGO films are shown in Figure 7-17. The eGO sheets in the films from regimes 1 and 2 exhibited their typical flatness on the substrate, with occasional wrinkles in the sheets. Although the overall deposition in regime 2 was spotty, in the locations where material deposited, the SEM imaging revealed that the film was continuous and free of microscale voids. The film from regime 3 appeared similar to its counterpart from the

15 V, 5 min experiments with a microstructure of multiple domains, each containing flat sheets, dominating the morphology.

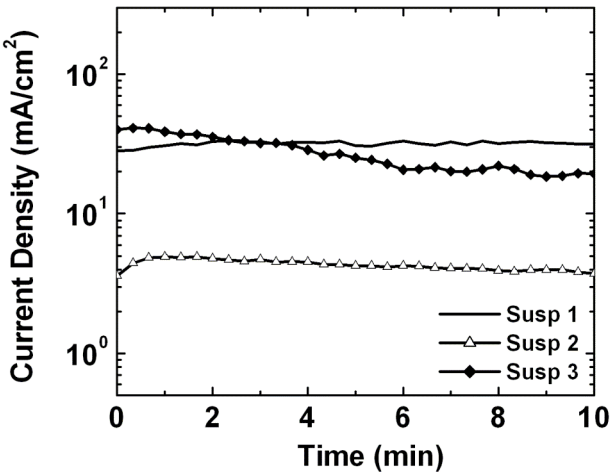

Figure 7-15. Normalized current during 15 V, 10 min experiments.

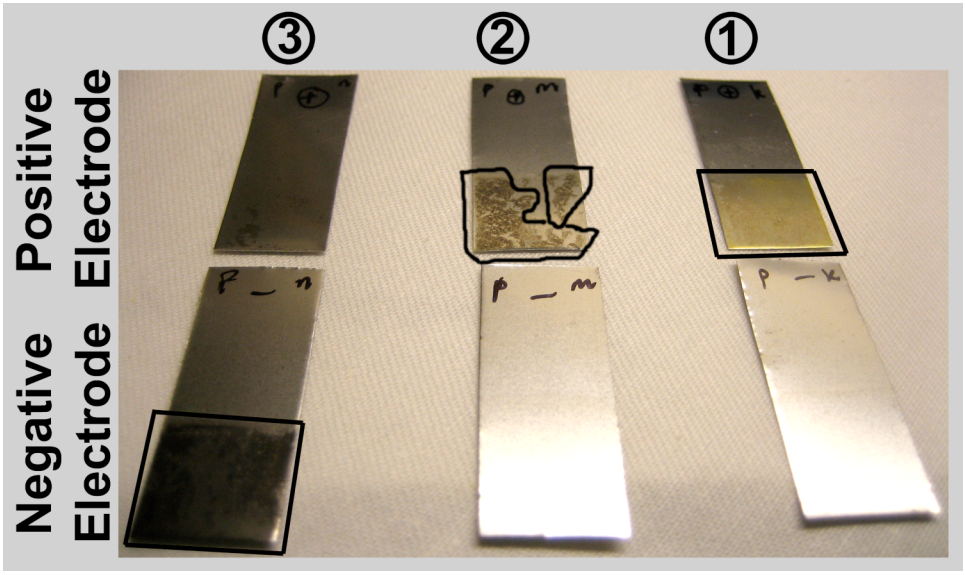

Figure 7-16. Photograph of electrodes from 15 V, 10 min experiments. Lines added as approximate guides to the film boundaries.

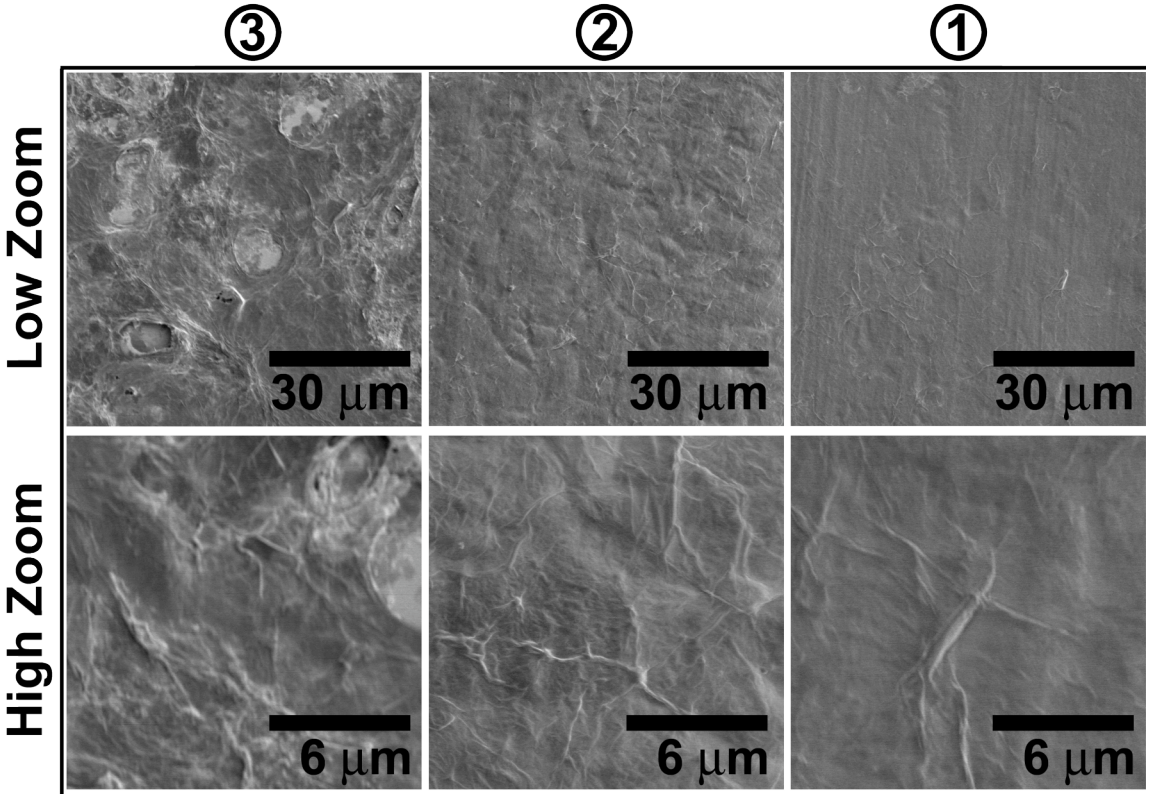

Figure 7-17. SEM images of the films formed in the 15 V, 10 min experiments. The film from suspension regime 3 was on the negative electrode, while the films from regimes 1 and 2 were on the positive electrode.

Table 7-5. Summary of 15 V, 10 min deposition experiment.

	Regime 3	**Regime 2**	**Regime 1**
Film Thickness	1,106 ± 172 nm ‡	Incomplete Film †	429 ± 49 nm †
Change in Suspension pH	+ 0.52	+ 0.74	- 0.19

‡ Film on negative electrode. † Film on positive electrode.

7.2.4 Comment on Thickness Measurements with Profilometer

Accurate measurements of the thickness of a substrate-bound film using profilometry require a defined step edge. Historically, for electrophoretically deposited nanomaterial films, we have produced the step edge by wiping away a section of film using the tip of a wood applicator stick. In these experiments with eGO films, we noted that it was difficult to wipe away a section of

the films and expose the substrate. We attributed this difficulty to the size and flat geometry of the eGO sheets, which allowed them to have a larger area in contact with the substrate than a spherical nanoparticle and consequently a stronger van der Waals attractive interaction. If increased downward force was applied during the wiping, the increased pressure deformed the surface of the steel substrate by creating a trench. These trenches had depth in the range from 12 μm to 27 μm (measured by optical microscope with assistance from John Rigueur in the Dickerson group). Remnant film and deformation of the substrate (Figure 7-18) contributed to the large measurement errors reported for the thickness measurements.

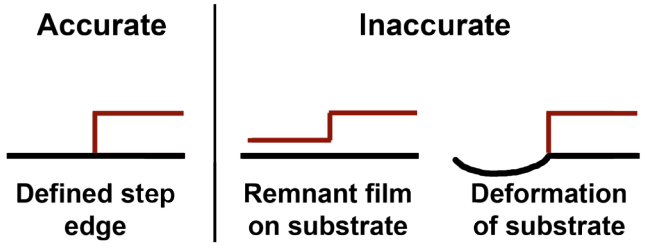

Figure 7-18. Accurate film thickness measurements using profilometry require a defined step edge between the substrate and the film. Inaccuracies result if film remains on the substrate or if the substrate is deformed.

7.3 Conclusions from Survey Experiments

Three different suspensions of eGO were used in a set of EPD survey experiments. The observed outcomes from these experiments were reported in the previous section. In this section, we summarize the results and discuss the implications of these findings.

Experiments were performed using applied dc voltages of 0.5 V, 3 V, and 15 V. From the measurements of current during EPD, we inferred that electrolysis of water occurred in the experiments using 3 V and 15 V. In some of the EPD runs, typically with currents higher than 10 mA/cm^2, the generation of H_2 and O_2 gas occurred at a sufficiently fast rate to produce visible bubbles. Given our knowledge of EPD mechanisms (Chapter 3), the electrolysis of water with its associated ion generation and consumption facilitated the aggregation of eGO sheets during the deposition process.

In all three suspensions, the zeta potential values were negative, indicating that the eGO sheets were negatively charged. During EPD, we expected that the sheets would move toward the positive electrode, where their deposition would be facilitated by the generation of H+ ions, which would screen the colloids' negative charges and reduce their electrostatic repulsion. In the low voltage experiments (3 V), we observed deposition of material on the positive electrode. The amount of material that deposited was proportional to the magnitude of the zeta potentials: regime 1 (-35.0 mV) and regime 2 (-33.4 mV) yielded complete films (regime 1 film ~ 4× thicker than regime 2 film) while regime 3 (-25.7 mV) yielded an incomplete film. This finding is reasonable, considering that zeta potential is proportional to electrophoretic mobility (Equation 2.5). Particles with lower magnitude zeta potential have lower mobility, meaning they move more slowly in a given electric field than particles with higher magnitude zeta potential. For a fixed voltage and time duration, material of lower magnitude zeta potential would move toward the electrode in a lesser quantity than material of higher magnitude zeta potential.

In the high voltage experiments (15 V), we anticipated an increase in the amount of eGO depositing on the positive electrode compared to their 3 V counterparts. For suspension regime 1, observation matched expectation, as a thicker film deposited on the positive electrode. For suspension regime 2, we observed patches of film rather than a film completely covering the positive electrode. We attributed the decrease in deposited material to three factors working in tandem: the eGO sheets' mobility (slightly lower compared to regime 1), the conductivity of the suspension (more than 15× lower than regimes 1 and 3), and the faster rate of generation of H+ ions at the positive electrode (compared to 3 V experiment). The lower mobility and conductivity meant that sheets moved more slowly toward the positive electrode. As the H+ ions diffused away from the positive electrode, their interaction with the eGO sheets further reduced the sheets' zeta potential magnitude and mobility toward the positive electrode. Their interaction with the eGO sheets also screened the Coulomb repulsion between sheets, leading to increased aggregation of the sheets. The observation that the suspension had flocculated by the end of the 15 V EPD runs provided further evidence for this progression of events.

The generation of H+ ions and their diffusion away from the positive electrode were crucial to the deposition observed at 15 V from suspension regime 3. When 15 V was applied to regime 3, eGO deposited in a few patches on the positive electrode but over the entire submerged area on the negative electrode. We attributed this behavior to a reversal of the charge on the eGO sheets. Colloids in regime 3 had the lowest zeta potential magnitude (and lowest electrophoretic mobility) of the three suspension regimes. As H+ ions interacted with the eGO sheets, they reduced the sheets' zeta potential magnitude and mobility toward the positive electrode, similarly to what was observed in regime 2. Because these sheets started with zeta potential closer to zero, the H+ ions were able to shift the zeta potential beyond zero to a positive value, giving the particles mobility toward the negative electrode. An EPD time of 5 min yielded a spotty deposit on the negative electrode, but 10 min sufficed to produce a continuous film over the negative electrode.

The deposition behavior detailed thus far had implications for the morphology of the films that were produced. Films deposited on the positive electrode appeared to possess continuous, constant-height regions of eGO sheets predominantly lying flat (parallel to the electrode surface). This morphology suggested that the eGO sheets arrived at the electrode individually and then began stacking to form the deposit. We designated films with this morphology as the "rug films" because their flat-but-occasionally-wrinkled morphology evoked the image of a throw rug whose one end had been pushed inward resulting in a small crease near the center of the rug. In contrast, the films deposited on the negative electrode, having passed through zero zeta potential to a positive value, appeared to possess microscale domains of flat eGO sheets with these domains stacked to different heights. The presence of these domains suggested the formation of face-to-face adhering multilayers of sheets prior to arrival at the negative electrode. We designated films with this morphology as the "brick films" because the domains at different heights in an otherwise continuous film resembled a slightly uneven brick walkway. Figure 7-19 provides a schematic for the formation of the rug and brick films. In both films, the eGO sheets were oriented with their large surfaces parallel to the electrode surface. This arrangement was

facilitated by the strong van der Waals interaction between planar surfaces and by the flow of solvent across the electrode surface.

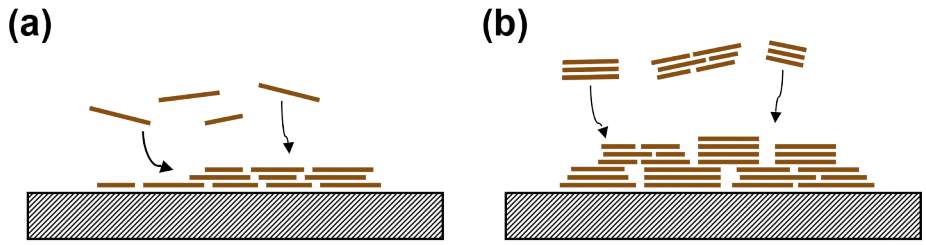

Figure 7-19. Schematic of (a) rug and (b) brick eGO film deposition. During rug film deposition, eGO sheets arrived individually at the electrode. During brick film deposition, eGO sheets arrived at the electrode as multilayered stacks. The multilayered stacks formed as a result of charge screening by H+ ions, per Figure 7-13.

We anticipated that the two distinct film morphologies would manifest themselves in the bulk properties of the film, such as surface wettability. Thus, we selected two sets of parameters to use as we investigated the preparation of free-standing eGO films by use of a sacrificial polymer.

(1) For rug films: Suspension regime 1 … 3 V, 15 min

(2) For brick films: Suspension regime 3 … 15 V, 10 min

Multiple parameters produced rug films, but using 3 V would minimize Joule heating that could damage the thin polymer sacrificial layer. The time was increased to 15 min since the 5 min deposition yielded films thinner than 300 nm. We targeted the production of thicker films to reduce the chance that they would be too fragile for handling and measurements. For the brick films, the same set of parameters used to produce a continuous film in the survey experiments would be used, since the films were thicker than 1,000 nm.

Having surveyed the EPD behavior of three different eGO suspension regimes using varied voltage and time parameters, we identified two distinct film morphologies (rug and brick) and associated deposition mechanisms. In the next chapter, we describe the effort to further

characterize the rug and brick eGO films and to prepare them as free-standing structures using the previously described sacrificial layer electrophoretic deposition technique.